

# Validity condition of separating dispersion of PCFs into material dispersion and geometrical dispersion

Wei Wang (王伟)<sup>1,2\*</sup>, Lantian Hou (侯蓝田)<sup>1,2</sup>, Zhaolun Liu (刘兆伦)<sup>1</sup>,  
and Guiyao Zhou (周桂耀)<sup>1,2</sup>

<sup>1</sup>Institute of Infrared Optical Fibres and Sensors, Yanshan University,  
Qinhuangdao 066004, China

<sup>2</sup>Key Laboratory of Metastable Materials Science and Technology, Yanshan University,  
Qinhuangdao 066004, China

\*E-mail: ysuwangwei@yahoo.com.cn

Received December 8, 2008

When using normalized dispersion method for the dispersion design of photonic crystal fibers (PCFs), it is vital that the group velocity dispersion of PCF can be seen as the sum of geometrical dispersion and material dispersion. However, the error induced by this way of calculation will deteriorate the final results. Taking 5 ps/(km·nm) and 5% as absolute error and relative error limits, respectively, the structure parameter boundaries of PCFs about when separating total dispersion into geometrical and material components is valid are provided for wavelength shorter than 1700 nm. By using these two criteria together, it is adequate to evaluate the simulated dispersion of PCFs when normalized dispersion method is employed.

OCIS codes: 060.2310, 060.5295, 060.4005.

doi: 10.3788/COL20090709.0768.

Photonic crystal fiber (PCF)<sup>[1,2]</sup> is a new kind of fiber whose cladding is composed of silica and periodic air holes. To define its geometrical structure, two parameters are needed, namely air hole diameter  $d$  and hole-to-hole pitch  $\Lambda$ . By tuning these two parameters, PCFs with different properties, such as broadband flatten dispersion<sup>[3–6]</sup> and dispersion compensation to conventional step index fiber (SIF)<sup>[7–10]</sup>, can be obtained. However, the flexibility of the structure tuning also results in the complexity of fiber design and makes the PCF design a time consuming process<sup>[11–13]</sup>. In order to simplify the dispersion design procedure, normalized dispersion method<sup>[14]</sup> was proposed by Kim *et al.* Dispersion flattened PCF and broadband dispersion compensating PCF have been achieved by using this method<sup>[15–17]</sup>. Through many numerical methods, the material dispersion of silica in the form of Sellmeier's equation can now be incorporated conveniently in the simulation. To employ the normalized dispersion method, the total dispersion  $D$  of PCFs must be seen as the sum of geometrical dispersion  $D_g$  and material dispersion  $D_m$ . However, the error induced by this way of calculation may sometimes deteriorate the final dispersion curve of the designed PCFs. So it is essential to find out the criterion with which the error induced by separating  $D$  of PCFs into  $D_g$  and  $D_m$  is acceptable.

In this letter, using an accurate full-vector method – multi-pole method (MPM), the group velocity dispersion (GVD) of PCFs with different structures is computed by including material dispersion directly and indirectly respectively, and the divergence between two ways of dispersion calculation is analyzed. Using the absolute error  $\Delta D=5$  ps/(km·nm) and relative error  $R_D=5\%$  as acceptable error limits, the criteria when separating the dispersion of PCFs into  $D_m$  and  $D_g$  is valid are provided.

We investigate the influences of the number of cladding

air hole layers on our simulation. For this purpose, a lossy model with the hole-to-hole pitch  $\Lambda=2.3$   $\mu\text{m}$ , the ratio of air hole diameter to hole-to-hole pitch  $d/\Lambda=0.2$  is simulated, and the index of non-dispersive core is assumed to be 1.45 for all the simulation below. We call the dispersion calculated through incorporating the material dispersion directly as  $D_{\text{dir}}$ , and the dispersion calculated as the sum of geometrical and material components as  $D_{\text{indir}}$ . Figure 1(a) shows  $D_{\text{dir}}$  and  $D_{\text{indir}}$  of the PCFs with 4 or 12 layers of cladding air holes. Figure 1(b) shows the absolute error  $\Delta D=|D_{\text{dir}}-D_{\text{indir}}|$  as a function of wavelength. From Fig. 1(b), it can be seen that at short wavelength, the divergence  $\Delta D$  is very small, while after a certain divergence wavelength  $\lambda_{\text{div}}$ , it begins to increase rapidly. The reason is that at short wavelength, the relative fiber core diameter to wavelength  $(2\Lambda-d)/\lambda$  is large compared with that at long wavelength, and light is confined tightly in the core area. The influence of geometrical structure on total dispersion  $D$  is very weak.  $D_g$  can be seen as the perturbation of  $D$ . With the increment of wavelength, light begins to interact with the fiber cladding, and  $D_g$  is too strong to be seen as perturbation. The wavelength  $\lambda_{\text{div}}$  at which  $\Delta D$  begins to increase is almost the same for PCFs with 4 and 12 layers of cladding air holes. Though the guiding mechanism of this kind of PCF is called modified total reflection, we must keep in mind that the guidance is actually the result of multi-scattering of light at the interface between air holes and silica. The extra rings of air hole can ensure more light to be scattered back to the core, however, it has no impact on when light begins to “sense” the cladding, which is exclusively determined by  $\Lambda$  and  $d$ . Thus,  $\lambda_{\text{div}}$  is determined mainly by the core diameter  $2\Lambda-d$  and relative air-hole diameter (also called the air-filling fraction)  $d/\Lambda$ .

The values of  $D_{\text{dir}}$  and  $D_{\text{indir}}$  are calculated for  $d/\Lambda=0.5$ ,  $\Lambda=1.5, 2.0, 2.5$   $\mu\text{m}$  and for  $\Lambda=2.3$   $\mu\text{m}$ ,  $d/\Lambda$

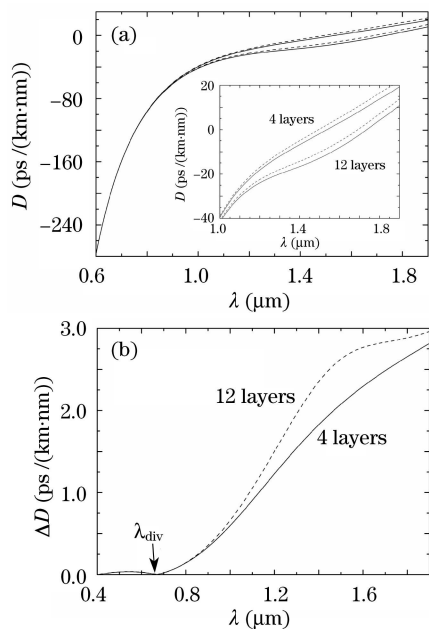


Fig. 1. (a) Dispersion  $D$  for PCFs with  $\Lambda=2.3 \mu\text{m}$ ,  $d/\Lambda=0.2$ , and 4 or 12 layers of cladding air holes, calculated by incorporating the material dispersion directly (solid line) and indirectly (dashed line). The inset shows the longer wavelength part. (b) Divergence  $\Delta D$  as a function of wavelength for 4 (solid line) and 12 (dashed line) layers of air holes.

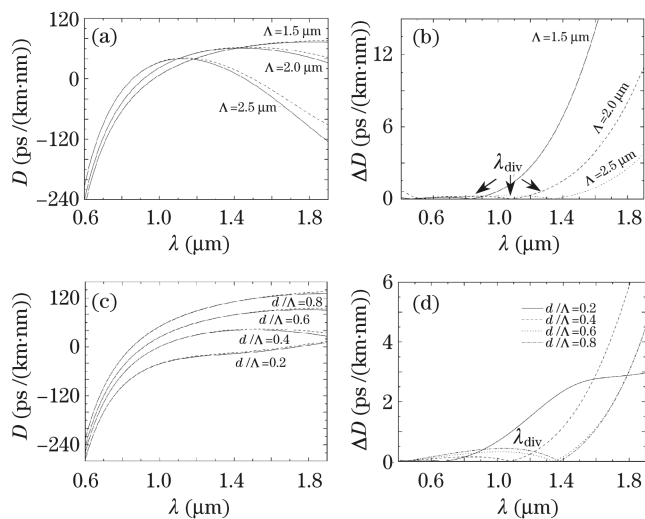


Fig. 2. (a) Dispersion  $D$  for PCFs with  $d/\Lambda=0.5$ ,  $\Lambda=1.5, 2.0, 2.5 \mu\text{m}$ , calculated by incorporating the material dispersion directly and indirectly. (b) Divergence  $\Delta D$  as a function of wavelength for  $\Lambda=1.5, 2.0,$  and  $2.5 \mu\text{m}$ . (c) Dispersion  $D$  for PCFs with  $\Lambda=2.3 \mu\text{m}$ ,  $d/\Lambda$  from 0.2 to 0.8 at a step of 0.2, calculated by incorporating the material dispersion directly and indirectly. (d) Divergence  $\Delta D$  as a function of wavelength for  $d/\Lambda=0.2, 0.4, 0.6,$  and  $0.8$ .

from 0.2 to 0.8 at a step of 0.2, respectively. The results are shown in Fig. 2. The number of air hole rings is chosen that all the PCFs simulated below have reasonable low loss. As seen from Fig. 2(b), given a certain  $d/\Lambda$ , a larger  $\Lambda$  means a larger core area, which guarantees stronger confinement ability of light and results in a longer divergence wavelength  $\lambda_{\text{div}}$ . When the hole-to-hole pitch  $\Lambda$  is set to be a constant, and

the air-filling fraction is changed, the situation becomes more complicated (Fig. 2(d)). At a given  $\Lambda$ , the increment of air-filling fraction results in the decrement of core diameter and the increment of surface between air holes and silica. The former factor goes against the light confinement and the latter is of benefit to light confinement. When the air-filling fraction is relatively low, the influence of air-filling fraction's increment is stronger than that of the core diameter's decrement. While the air-filling fraction is larger, the influence of core diameter's decrement gets stronger. It balances, even surpasses the impacts of air-filling fraction's increment. This can be clearly seen from Fig. 2(d): the larger the air-filling fraction is, the longer the  $\lambda_{\text{div}}$  is. However, for large air-filling fraction, this trend is not so obvious. Though not shown in Fig. 2(d), when the air-filling fraction is large enough, the trend even reverses. The value of  $\Delta D$  for  $d/\Lambda=0.2$  increases slowly after about  $1.4 \mu\text{m}$ . A small air-filling fraction means a tiny index

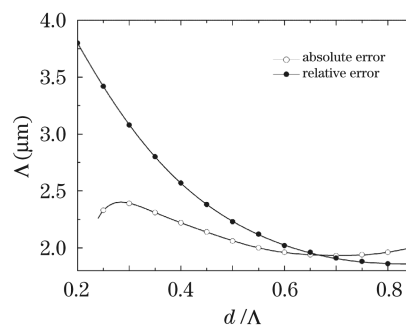


Fig. 3. Structure parameter boundaries for absolute error and relative error.  $\Delta D$  is always smaller than  $5 \text{ ps}/(\text{km}\cdot\text{nm})$  for  $d/\Lambda < 0.24$ .

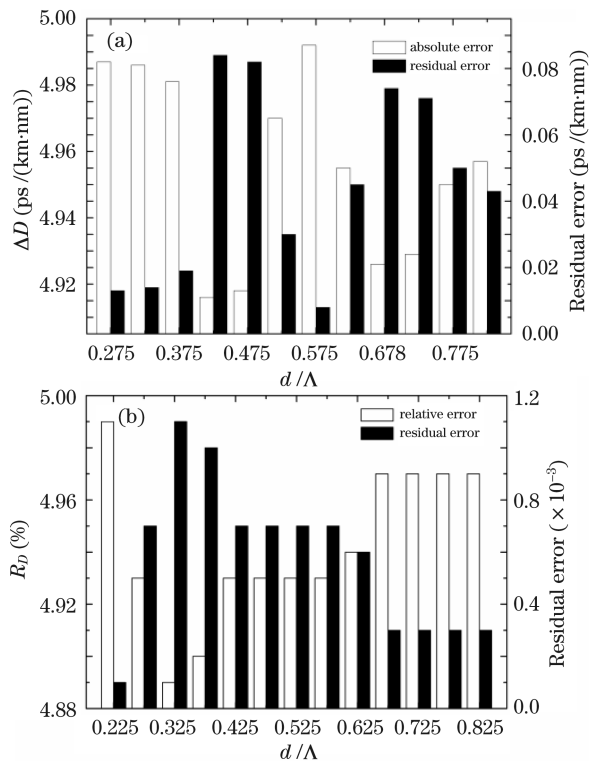


Fig. 4. (a) Precision of absolute error  $\Delta D$  at  $d/\Lambda$  from 0.275 to 0.825 at a step of 0.05; (b) precision of relative error  $R_D$  at  $d/\Lambda$  from 0.225 to 0.825 at a step of 0.05.

**Table 1. Coefficients of Polynomial Fitting for  $\Delta D$  and  $R_D$  Error Limits**

	For $\Delta D$	For $R_D$	For $\Delta D$	For $R_D$
$(d/\Lambda)^9$	21305.792	—	$(d/\Lambda)^4$	-169708.670 -278.915
$(d/\Lambda)^8$	-113724.565	—	$(d/\Lambda)^3$	62032.366 181.668
$(d/\Lambda)^7$	266054.875	—	$(d/\Lambda)^2$	-14326.743 -51.249
$(d/\Lambda)^6$	-357695.003	-62.608	$(d/\Lambda)^1$	1895.416 -1.947
$(d/\Lambda)^5$	304277.745	209.629	$(d/\Lambda)^0$	-106.840 5.170

**Table 2. Examples of Employing the Error Limits to PCFs with Varied Cladding Air Holes**

	$\Lambda$ ( $\mu\text{m}$ )	$d_1/\Lambda$	$d_2/\Lambda$	$d_3/\Lambda$	$d_4/\Lambda$	$d_5/\Lambda$	Maximal Error
Fiber 1*	1.96	0.80	0.8	0.65	0.65	0.65	4.9685
Fiber 2*	2.22	0.40	0.45	0.45	0.50	0.50	3.9746
Fiber 3**	1.91	0.70	0.75	0.80	0.85	—	4.62%
Fiber 4**	1.91	0.85	0.80	0.75	0.70	—	4.45%

$d_i$  represents the  $i$ th inner cladding air hole. \* and \*\* represent the fibers that satisfy the absolute error and relative error limits, respectively.

difference between core and cladding, which guarantees the satisfaction of weakly guided convention. Also, the zero-dispersion wavelength  $\lambda_{\text{zero}}$  of PCF is important for some nonlinear applications. From Figs. 2(a) and (c), we can see that for most situations,  $\lambda_{\text{zero}}$  is longer than  $\lambda_{\text{div}}$ . Thus, separating total  $D$  into  $D_g$  and  $D_m$  hardly changes the position of  $\lambda_{\text{zero}}$ . However, when  $\lambda_{\text{zero}}$  is shorter than  $\lambda_{\text{div}}$  (see the inset of Fig. 1(a)), separating total  $D$  into  $D_g$  and  $D_m$  will induce several tens nanometers shift of  $\lambda_{\text{zero}}$ .

To employ the normalized dispersion method for PCF design, it is necessary to evaluate the error induced by separating  $D$  into  $D_g$  and  $D_m$ . From the analysis above, we know that the longer the wavelength is, the larger the absolute and relative errors are. Practically, considering the current application and future band expansion in an optical communication system (the upper wavelength of L band is 1625 nm), we set 1700 nm as the upper wavelength limit and  $\Delta D = |D_{\text{dir}} - D_{\text{indir}}| = 5$  ps/(km·nm),  $R_D = \Delta D / |D_{\text{dir}}| = 5\%$  as absolute and relative error limit to provide the criteria of when separating  $D$  into  $D_g$  and  $D_m$  is acceptable. Firstly, the appropriate values of hole to hole pitch  $\Lambda$  (the precision of  $\Lambda$  is 0.01  $\mu\text{m}$ ) are found out for  $d/\Lambda$  from 0.2 to 0.85 at a step of 0.05. Due to the small index difference between core and cladding, for all the PCF structures with  $d/\Lambda$  less than 0.24,  $\Delta D$  is smaller than 5 ps/(km·nm). According to the definition of  $R_D$ , the value of  $R_D$  will go meaninglessly high around zero dispersion wavelength. However, the divergence is actually very small. So, these meaningless values around zero dispersion wavelength have been omitted. Then, by polynomial fitting of the data points, the absolute error and relative error limit boundaries are obtained, as shown in Fig. 3 and Table 1. In Fig. 3, the structure parameters' space above the curves is the valid zone to separate  $D$  into  $D_g$  and  $D_m$  for the wavelength shorter

than 1700 nm. The accuracies of the criteria are also verified at  $d/\Lambda = 0.275$  to 0.825 for absolute error and  $d/\Lambda = 0.225$  to 0.825 for relative error at a step of 0.05 (Fig. 4). The residual error is very small, which indicates the validity of these two criteria. Also, these two criteria can be extended to some PCFs with varied cladding air holes only if the structure parameters are all in the upper or lower part of Fig. 4(a). Table 2 gives some examples of employing the criteria to PCFs with varied cladding holes.

In conclusion, by taking 1700 nm as the wavelength upper limit, 5 ps/(km·nm) and 5% as absolute error and relative error limits, respectively, two criteria are provided about when separating  $D$  of PCFs into  $D_m$  and  $D_g$  is valid. When using the normalized dispersion method to design the dispersion properties, by individually or combinedly using these two criteria, we believe that it is adequate to evaluate the error of all the simulated results.

This work was supported by the National Natural Science Foundation of China (No. 60637010) and the Science Foundation of Yanshan University for the Excellent PhD Students.

## References

1. J. C. Knight, T. A. Birks, P. St. J. Russell, and D. M. Atkin, *Opt. Lett.* **21**, 1547 (1996).
2. T. Sun, G. Kai, Z. Wang, S. Yuan, and X. Dong, *Chin. Opt. Lett.* **6**, 93 (2008).
3. K. Saitoh, M. Koshiba, T. Hasegawa, and E. Sasaoka, *Opt. Express* **11**, 843 (2003).
4. G. Renversez, B. Kuhlmeiy, and R. McPhedran, *Opt. Lett.* **28**, 989 (2003).
5. T.-L. Wu and C.-H. Chao, *IEEE Photon. Technol. Lett.* **17**, 67 (2005).
6. J. Wang, C. Jiang, W. Hu, and M. Gao, *Opt. Laser Technol.* **38**, 169 (2006).
7. A. Huttunen and P. Törmä, *Opt. Express* **13**, 627 (2005).
8. S. K. Varshney, T. Fujisawa, K. Saitoh, and M. Koshiba, *Opt. Express* **13**, 9516 (2005).
9. S. K. Varshney, T. Fujisawa, K. Saitoh, and M. Koshiba, *Opt. Express* **14**, 3528 (2006).
10. M. Wu, D. Huang, H. Liu, and W. Tong, *Chin. Opt. Lett.* **6**, 22 (2008).
11. S. K. Varshney, K. Saitoh, and M. Koshiba, *IEEE Photon. Technol. Lett.* **17**, 2062 (2005).
12. Q. Fang, Z. Wang, L. Jin, J. Liu, Y. Yue, Y. Liu, G. Kai, S. Yuan, and X. Dong, *J. Opt. Soc. Am. B* **24**, 2899 (2007).
13. H. Subbaraman, T. Ling, Y. Jiang, M. Y. Chen, P. Cao, and R. T. Chen, *Appl. Opt.* **46**, 3263 (2007).
14. J. Kim, U.-C. Paek, D.Y. Kim, and Y. Chung, in *Optical Fiber Communication Conference 2001 OSA Technical Digest WDD86* (2001).
15. A. Ferrando, E. Silvestre, P. Andrés, J. J. Miret, and M. V. Andrés, *Opt. Express* **9**, 687 (2001).
16. L. P. Shen, W.-P. Huang, G. X. Chen, and S. S. Jian, *IEEE Photon. Technol. Lett.* **15**, 540 (2003).
17. L.-P. Shen, W.-P. Huang, and S.-S. Jian, *J. Lightwave Technol.* **21**, 1644 (2003).